RM No. A8L20

RESEARCH MEMORANDUM

INVESTIGATION OF A THIN STRAIGHT WING OF ASPECT RATIO 4 BY THE NACA WING-FLOW METHOD.- LIFT AND PITCHING-MOMENT CHARACTERISTICS OF THE WING ALONE

By George A. Rathert, Jr., Carl M. Hanson,
and L. Stewart Rolls

Ames Aeronautical Laboratory
Moffett Field, Calif.

NATIONAL ADVISORY COMMITTEE
FOR AERONAUTICS

WASHINGTON
February 14, 1949

Classification cancelled (or changed to Unclassified
By Authority NASA Tech... Announcement ...
(OFFICER AUTHORIZED TO CHANGE) 06 Jan 64

By

GRADE OF OFFICER MAKING CHANGE)

11 Apr 61
DATE

NACA RM No. A8L20

[redacted]

NATIONAL ADVISORY COMMITTEE FOR AERONAUTICS

RESEARCH MEMORANDUM

INVESTIGATION OF A THIN STRAIGHT WING OF ASPECT RATIO 4 BY THE NACA WING-FLOW METHOD.- LIFT AND PITCHING-MOMENT CHARACTERISTICS OF THE WING ALONE

By George A. Rathert, Jr., Carl M. Hanson,
and L. Stewart Rolls

SUMMARY

The lift and pitching-moment characteristics of a straight wing of aspect ratio 4, taper ratio 0.5, having a symmetrical double-wedge airfoil section with a maximum thickness of 4.4-percent chord, have been measured by the NACA wing-flow method in the Mach number range 0.51 to 1.20 and the Reynolds number range 380,000 to 660,000. The results are compared with theory and with wind-tunnel tests of a similar model.

Below 0.82 Mach number, the lift-curve slope was not affected by surface condition and could be computed quite accurately by using the Weissinger lifting-line method. Above 0.82 Mach number, the lift-curve slope increased more abruptly than indicated by theory, reached a peak at 0.92 Mach number, then gradually decreased thereafter at a lower rate than indicated by Lagerstrom's lifting-surface theory for supersonic speeds. In the Mach number range of 0.82 to 1.00, both the lift and pitching-moment characteristics were considerably affected by the surface condition, and, presumably, the test Reynolds number.

The pitching-moment-curve slopes indicated that up to 0.83 Mach number the aerodynamic center remained at approximately 0.25 M.A.C. in general agreement with theory and wind-tunnel tests. Between 0.83 and 1.20 the aerodynamic center moved rearward to 0.42 M.A.C., approaching the supersonic theoretical curve.

[redacted]

INTRODUCTION

The NACA wing-flow method is currently being used to study the effects of Mach number on the lift-curve slope and aerodynamic center of several types of wing plan forms suitable for transonic or supersonic flight. This report presents the results for the first plan form tested, a straight wing of aspect ratio 4, taper ratio 0.5, having a symmetrical double-wedge airfoil section with a maximum thickness of 4.4-percent chord.

The primary purpose of the test program is to determine if any abrupt or excessive changes occur in the transonic speed range; however, the results are also used to investigate the extent to which the characteristics can be predicted theoretically and to evaluate the testing technique by providing direct comparison with wind-tunnel data at higher Reynolds numbers. The semispan wing was designed as a 1/9-scale model of a wing tested in the Ames 12-foot pressure wind tunnel (reference 1), the source of the comparative data.

SYMBOLS

A_X	ratio of the net aerodynamic force along the test vehicle X axis (positive when directed forward) to the weight of the test vehicle
C_L	lift coefficient $\left(\frac{\text{lift}}{qS'}\right)$
C_m	pitching-moment coefficient, used with subscript to denote longitudinal reference axis $\left(\frac{\text{pitching moment}}{qS'\bar{c}}\right)$
M	Mach number $\left(\frac{V}{a}\right)$
R	Reynolds number $\left(\frac{\rho V c}{\mu}\right)$
S'	wing area of the semispan model, square feet
V	airspeed, feet per second
a	speed of sound, feet per second
b	wing span, feet

c	local chord, feet
$\bar{c}$	mean aerodynamic chord $\left(\frac{\int_0^{b/2} c^2 dy}{\int_0^{b/2} c\, dy}\right)$, feet
c_r	root chord, feet
q	dynamic pressure $\left(\frac{1}{2}\rho V^2\right)$, pounds per square foot
u	local velocity, feet per second
y	spanwise location, feet
z	distance above test-station surface, inches
α	angle of attack, degrees
δ	boundary-layer thickness, inches
δ^*	displacement thickness $\left\{\left[\int_0^{\delta}\left(1 - \frac{\rho u}{\rho_\delta \mu_\delta}\right)\right] dz\right\}$, inches
μ	air viscosity, slugs per foot-second
ρ	mass density of air, slugs per cubic foot

Subscripts

$o.25\bar{c}$	25-percent M.A.C. reference axis
$o.50\bar{c}$	50-percent M.A.C. reference axis
δ	edge of boundary layer

TEST EQUIPMENT

The data were obtained by placing the semispan model in a region of accelerated air flow over a special built-up test station on an airplane wing. The model was mounted normal to the test-station surface on a three-component recording balance which was oscillated continuously to vary the angle of attack. A view of the test station with the model installed is given in figure 1.

Model

The model was a 1/9-scale reproduction of the one described in reference 1 and was constructed of solid steel. Practical machining tolerances, which were expended mainly to keep the model symmetrical, resulted in the dimensions indicated in the drawing of the model (fig. 2). The only significant difference between the wind-tunnel and wing-flow models was a reduction of 0.1 percent in thickness ratio which should primarily have affected the drag data. The measurements were made to an accuracy of ±0.0002 inch. Figure 3 is a photograph of the model.

Balance

The three-component balance (normal force, chord force, and pitching moment) is illustrated schematically in figure 4. The top of the balance, which is 6 inches in diameter and serves as the model end plate, is supported by four side posts in such a manner that it is prevented from tilting by the side posts but restrained from translation and rotation by the appropriate strain-gage members only. Flow from the interior of the wing through the gap to the wing surface is impeded by a three-element baffle with clearances of 0.015 inch. The model angle of attack is varied by rotating the entire balance assembly at a rate of 1° per second. The fixed and rotatable parts are indicated in figure 4.

The strain-gage elements are enclosed in a thermally insulated drum containing a heat supply and regulator intended to maintain a constant operating temperature. The gage outputs are recorded by standard NACA double-element galvanometers synchronized at half-second intervals by an electric chronometer. The galvanometers and the current regulators are also maintained at the operating temperature of the gages in the balance chamber.

Flow Field

Measured characteristics of the flow field include the horizontal and the vertical Mach number gradients and test-station boundary-layer profile. The measurements were made without the model in place but under conditions of constant airplane Mach number, normal acceleration, and average pressure altitude otherwise identical with the test runs.

The streamwise or chordwise Mach number distributions were computed from the static pressure on the test-station surface and the free-stream stagnation pressure. These data (fig. 5) indicate that the chordwise Mach number gradient on the model was less than 0.01 per inch at a test Mach number of 1.20. This gradient falls off to zero at the lower Mach numbers.

The vertical (spanwise on the model) Mach number gradients were studied indirectly on a similar test station by recording total and static pressures at the 60-percent-chord point on a 10-inch-high wedge-shaped airfoil and computing the spanwise variation of local Mach number on the wedge. According to these data (fig. 6), the Mach number decreased approximately 0.01 for each inch of model span, and the gradient was relatively independent of test Mach number. Direct measurements of a vertical static pressure field showing results consistent with those presented here are discussed in reference 2.

Typical test-station boundary-layer profiles are presented in figure 7. These data were obtained by the methods described in reference 3 and used to compute the boundary-layer displacement thickness, 0.045 inch at a test-station Mach number of 1.15. The ratio of displacement thickness to model height was 0.011 which is comparable with the value of 0.014 for the tests of reference 1.

The values of Mach number and dynamic pressure at the model centroid of area were determined from the preceding gradients and used in the reduction of the test data. The corresponding average variation of model Reynolds number with test Mach number (fig. 8) was computed by assuming isentropic expansion from free-stream stagnation conditions to the test station at a pressure altitude of 15,000 feet.

ACCURACY

Deviations in the experimental results from the correct full-scale free-flight characteristics may arise from three sources: (1) uncertainties in the direct physical measurements, (2) measurement errors introduced by aerodynamic effects (e.g., the effect of the presence of the model on the flow field), and (3) actual changes in aerodynamic characteristics resulting from differences in scale.

Data precision is normally defined in terms of just the first two sources of error; however, in tests of the present type the unknown scale effects may be quite large and cannot be separated experimentally from the errors. It is possible to treat individually only the direct physical measuring equipment and its accuracy, which is the subject of this section.

Mach Number

The results of the calibration runs indicate that the over-all uncertainty in Mach number is ±2.0 percent. This figure includes variations from flight to flight and also within the 10-second period in which the records are obtained. The corresponding uncertainty in dynamic pressure varies from ±3.4 to ±1.8 percent over the Mach number range.

Angle of Attack

The local flow direction was obtained by averaging the measured attitudes of the two free-floating reference vanes visible on either side of the model in figure 1. The angle of attack was computed from the positions of the reference vanes which were measured by a direct optical system with an accuracy of ±0.1° and the angular position of the model (corrected for moment-gage deflection) which was measured by an autosyn system with an accuracy of ±0.4°. The combined precision was therefore ±0.42°.

Force Measurements

The major uncertainty in the force measurements is a variation in the strain-gage zero-load readings under operating conditions. This uncertainty amounts to ±2.0 percent of the maximum load values, or ±0.06 pound normal force, ±0.02 pound chord force, and ±0.06 inch-pound pitching moment. The calibration slopes are not affected.

Tare Corrections

The following sources of tare loads were investigated: (1) friction in the balance assembly, (2) forces on the model and balance top due to static pressure gradients, (3) acceleration loads due to the weight of the model and balance top, (4) skin friction on the balance top or end plate, and (5) interaction between the normal- and

chord-force gages due to misalinement about the gage neutral axes. The first two effects were found to cause tare forces smaller than one-half of one percent of the maximum loads and have been neglected. Corrections for the last three effects were determined and have been applied as described in the following paragraphs. The corrections are all chord-force tares and amount to several times the magnitude of the basic drag forces. For this reason no drag data are presented and the corrections have been used only to compute C_L and $C_{m_{0.25c}}$

Acceleration.- The longitudinal acceleration of the test airplane produced a tare force in the streamwise direction equal to the product of A_X and the effective weight of the balance top and model assembly, 3.51 pounds. The tare corrections were computed from continuous measurements of A_X obtained from a sensitive accelerometer mounted parallel to the plane of the balance top.

Skin friction.- An additional streamwise tare force was produced by the skin friction acting on the relatively large area of the balance top. The skin-friction drag coefficient was measured during tests with no model in place and then applied to the area of the balance top exposed with the model installed to compute the tare force. At a test-station Mach number of 0.51 the skin-friction drag coefficient was 0.005, giving a tare force equal to a model drag coefficient of 0.0177 at zero angle of attack.

Misalinement.- The third correction found necessary was one applied to the chord-force data as a function of normal force to compensate for the misalinement of the chord-force gage about its neutral axis. The correction was determined from static-load calibration tests.

Summary of Accuracy

Almost all of the preceding errors are of a type that would be constant within one dive or one angle-of-attack sequence, which means that the accuracies presented apply principally to the determination of absolute values and that the measurement of slopes such as $dC_L/d\alpha$ should be more precise. This reasoning may be substantiated by comparing the relative amount of scatter in the plots of $dC_L/d\alpha$ with the scatter in C_L for $\alpha = 0$.

The effect of the preceding information will be illustrated by a table presenting examples of the absolute value and the uncertainty of the test data at the lowest and highest dynamic pressures and a lift coefficient of 0.50.

[redacted]

Quantity	M = 0.51	M = 1.20
Mach number, M	0.51 ± 0.01	1.20 ± 0.02
Angle of attack, α, degrees	7.3 ± 0.4	5.9 ± 0.4
Lift coefficient, C_L	0.500 ± 0.018	0.500 ± 0.009
Pitching-moment coefficient		
$C_{m_{o.50\bar{c}}}$	0.100 ± 0.005	0.047 ± 0.001
$C_{m_{o.25\bar{c}}}$	−0.023 ± 0.007	−0.077 ± 0.002
Drag coefficient, C_D	0.011 ± 0.004	0.030 ± 0.001

TESTS AND RESULTS

The model was tested with two surface conditions; polished smooth and coated with a mixture of clear lacquer and lampblack over the leading 50-percent-chord portion of both surfaces. The largest lampblack particles were 0.002-inch high.

The data were recorded in the form of time histories of an oscillation of the model from -2° to $+8^\circ$ angle of attack at constant Mach numbers ranging from 0.51 to 1.20. The corresponding Reynolds numbers may be found in figure 8. In order to obtain stable test data, the test-station Mach number was held constant and the model rotation started 3 to 5 seconds in advance of the period in which the data were used. Three typical time histories are presented in figure 9.

The lift and pitching-moment characteristics of the model with the polished surface are presented in figures 10 and 11. The characteristics of the roughened model are presented in figures 12 and 13. Tests of the roughened model with an extended angle-of-attack range to obtain stall detail at a Mach number of 0.88 are presented in figure 14. The pitching-moment data in figures 11, 13, and 14 have been transferred from the 0.50 M.A.C. axis of measurement to the 0.25 M.A.C. axis.

[redacted]

DISCUSSION

Examination of figures 10 and 12 shows that at all Mach numbers the lift varied linearly with angle of attack up to approximately 0.50 lift coefficient. The pitching-moment data (figs. 11 and 13) indicate an increase in stability or large rearward aerodynamic-center shift starting at lift coefficients of 0.30 to 0.40. Below this stable break the data were linear at all Mach numbers. The preceding characteristics were not affected appreciably by changing the surface condition.

Maximum lift was attained only on a few runs near the critical Mach number. Although the test Reynolds number is quite low, a representative time history of a complete stall is presented as a matter of interest in figure 9(b). The corresponding cross plots are presented in figure 14.

Effects of Mach Number

The effects of Mach number on the lift-curve and pitching-moment-curve slopes at zero lift are presented in figure 15. Symbols are used to indicate the individual slope measurements in order to show clearly the amount of scatter obtained in relation to the size of the changes discussed.

The lift-curve slope of the wing with polished surface increased smoothly up to 0.82 Mach number, then rose more abruptly to a maximum of 0.104 at 0.92 Mach number, an increase of about 50 percent over the low-speed value. At higher Mach numbers the slope decreased gradually up to the limit test Mach number, 1.20. Adding surface roughness flattened out the abrupt rise between 0.82 and 0.92 Mach numbers so that the peak value was less and occurred at a higher Mach number. This effect will be discussed in more detail later.

The pitching-moment-curve slopes indicate that at low speeds the aerodynamic center was at the 0.25 M.A.C. point. There was relatively little change up to 0.83 Mach number when the aerodynamic center moved rearward to about 0.34 M.A.C. at 0.88 Mach number. In the Mach number range 0.88 to 0.95 there was a small reduction in stability, equivalent to a forward movement of 0.025 M.A.C. From 0.95 to 1.20 Mach number the aerodynamic center moved steadily to the rear to 0.42 M.A.C. at 1.20 Mach number. The result of adding surface roughness was the same as in the case of the lift-curve slope, affecting the data only in the Mach number range of 0.88 to 0.97.

[redacted]

Comparison with Wind-Tunnel Tests and Theory

The data are compared with the results of the Ames 12-foot pressure wind tunnel (reference 1) in figure 15, and with appropriate theory in figure 16. Two sets of the wind-tunnel data are presented in order to compare the effect of rounding of the midchord ridge lines with the addition of roughness in the wing-flow tests. For the theoretical calculations, the lifting-line method of Weissinger as applied in reference 4 was used in the subsonic range and corrected for compressibility as suggested in the reference. For the supersonic speed range, the results of Lagerstrom's lifting-surface theory were obtained from reference 5.

Lift-curve slope.- In figure 17 individual curves of the lift-coefficient variation with angle of attack for the wing-flow and the wind-tunnel tests show good agreement at 0.5 Mach number. Between 0.51 and 0.82 Mach numbers the wing-flow and wind-tunnel lift-curve slopes remain in very good agreement (fig. 15). Both the absolute value and the rate of increase with Mach number were predicted accurately by using the Weissinger method (fig. 16). Neither changing the surface condition in the wing-flow tests nor the ridge-line contour during the wind-tunnel tests had any significant effect on the lift-curve slopes.

From 0.82 to 0.93 Mach number the experimental slopes increased much faster than the theoretical value, and the amount of divergence from theory was appreciably affected by the surface condition and the ridge-line contour. This rise and subsequent peak in lift-curve slope is believed to be due to the effect of Mach number on the negative pressure peak associated with the sharp ridge line on the upper surface. Adding roughness, which thickens the boundary layer, and rounding of the ridge line tend to reduce this pressure peak. These modifications are seen in figure 15 to reduce the lift-curve-slope rise considerably. Also, the increase in lift-curve slope is accompanied by an equally abrupt rearward shift in the aerodynamic center which could be explained by the same increase in the midchord negative pressure peak.

The data of figure 15 indicate that the surface condition of the model continues to have a critical effect on the wing characteristics throughout the Mach number range 0.82 to 1.00. Whether or not the surface condition is critical because of the particular effect suggested on the ridge-line pressures, it seems apparent that viscous flow effects are involved. In the specified Mach number range, therefore, the model surface, profile, and test Reynolds number all would be very important considerations in any attempt to

[redacted]

study or predict full-scale characteristics from small-model tests.

The correlation between the wing-flow model with polished surface and the wind-tunnel model with sharp ridge lines is fairly good up to the peak value of lift-curve slope. Thereafter, however, the wind-tunnel model loses lift effectiveness much more rapidly. Again this difference in behavior is believed to be due to viscous and compressible flow effects. The presence of pressure peaks on both the upper and lower surfaces and the accompanying possibility that Mach number changes will affect each peak differently afford a good deal of opportunity for lack of agreement.

In the supersonic range there was no effect of the change in surface condition, but the agreement with theory (fig. 16) is not as satisfactory as in the subsonic case. The variation of lift-curve slope with Mach number was less than predicted theoretically, although the tests did not extend to a high enough Mach number to be really conclusive.

Aerodynamic center.- The correlation between wing-flow and wind-tunnel tests of the marked increase in stable pitching-moment-curve slope, or rearward aerodynamic center shift, starting at 0.40 lift coefficient was quite good, as illustrated in figure 17. The slopes of the pitching-moment curves at zero lift, figure 15, show only fair qualitative agreement with the wind-tunnel results. The wing-flow data indicate a more rearward aerodynamic center and a slight movement aft instead of forward with increasing Mach number. These discrepancies are comparable in size with the amount of scatter in the wing-flow data. Both the wind-tunnel and the wing-flow curves show the same increase in stability with Mach number associated with the abrupt rise in lift-curve slope.

At supersonic speeds the rearward movement of the aerodynamic center approached agreement with the theoretical value, as shown in figure 16. In the subsonic range the use of the lifting-line theory inherently places the center of pressure at the quarter-chord point.

CONCLUSIONS

NACA wing-flow method tests of a thin straight wing with a symmetrical double-wedge profile, and a comparison of the results with theory and larger scale wind-tunnel data have led to the following conclusions:

1. From 0.51 to 0.82 Mach number the lift-curve slope

increased smoothly and in good agreement with the wind-tunnel results. Both the absolute value and the rate of increase with Mach number were predicted accurately by using the Weissinger lifting-line method.

2. Above 0.82 Mach number the lift-curve slope of the model with polished surface abruptly increased more rapidly than indicated by theory, reached a maximum about 50 percent greater than the low-speed value at a Mach number of 0.92, and then decreased gradually at higher speeds.

3. Within the Mach number range 0.82 to 1.00 the lift and pitching-moment characteristics were considerably affected by the model surface condition and, by inference, the test Reynolds number. The effects of compressibility and viscosity on the negative pressure peaks associated with the midchord ridge lines are suggested as a possible explanation.

4. In the limited supersonic range covered by the tests, 1.00 to 1.20 Mach number, the lift-curve slope decreased less rapidly with increasing Mach number than predicted by the lifting-surface theory of Lagerstrom.

5. The pitching-moment-curve slopes indicate that up to 0.83 Mach number the aerodynamic center remained at approximately 0.25 M.A.C. in general agreement with theory and wind-tunnel tests. Between 0.83 and 1.20 the aerodynamic center moved rearward to 0.42 M.A.C., approaching the supersonic theoretical curve. The movement was gradual except for the Mach number range associated with the abrupt increase in lift-curve slope.

6. At all Mach numbers a marked increase in the stable pitching-moment-curve slopes occurred starting at 0.30 to 0.40 lift coefficient. This characteristic was also observed in the wind-tunnel tests.

Ames Aeronautical Laboratory,
National Advisory Committee for Aeronautics,
Moffett Field, California.

REFERENCES

1. Johnson, Ben H., Jr.: Investigation of a Thin Wing of Aspect Ratio 4 in the Ames 12-Foot Pressure Wind Tunnel. I - Characteristics of a Plain Wing. NACA RM No. A8D07, 1948.

2. Johnson, Harold I.: Measurements of Aerodynamic Characteristics of a 35° Sweptback NACA 65-009 Airfoil Model with 1/4-Chord Plain Flap by the NACA Wing-Flow Method. NACA RM No. L7F13, 1947.

3. Zalovcik, J. A., and Luke, E. P.: Some Flight Measurements of Pressure-Distribution and Boundary-Layer Characteristics in the Presence of Shock. NACA RM No. L8C22, 1948.

4. DeYoung, John: Theoretical Additional Span Loading Characteristics of Wings with Arbitrary Sweep, Aspect Ratio, and Taper Ratio. NACA TN No. 1491, 1947.

5. Lagerstrom, P. A., Wall, D., and Graham, M. E.: Formulas in Three-Dimensional Wing Theory. Douglas Aircraft Company Rep. No. SM11901, 1946.

[redacted]

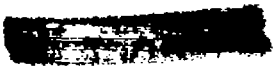

Figure 1.- The wing-flow test station with the model installed.

[redacted]

[redacted]

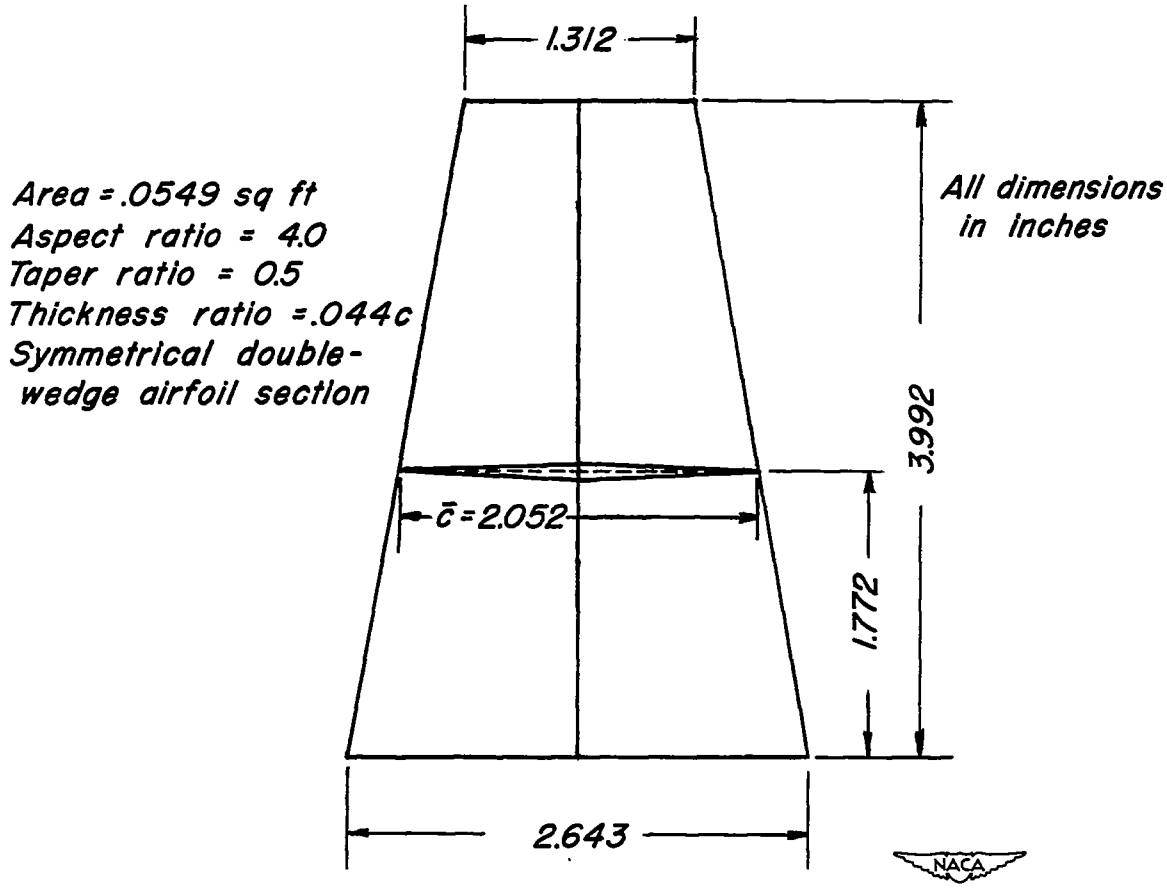

Figure 2.- Dimensions of model.

[redacted]

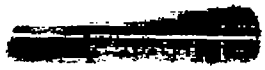

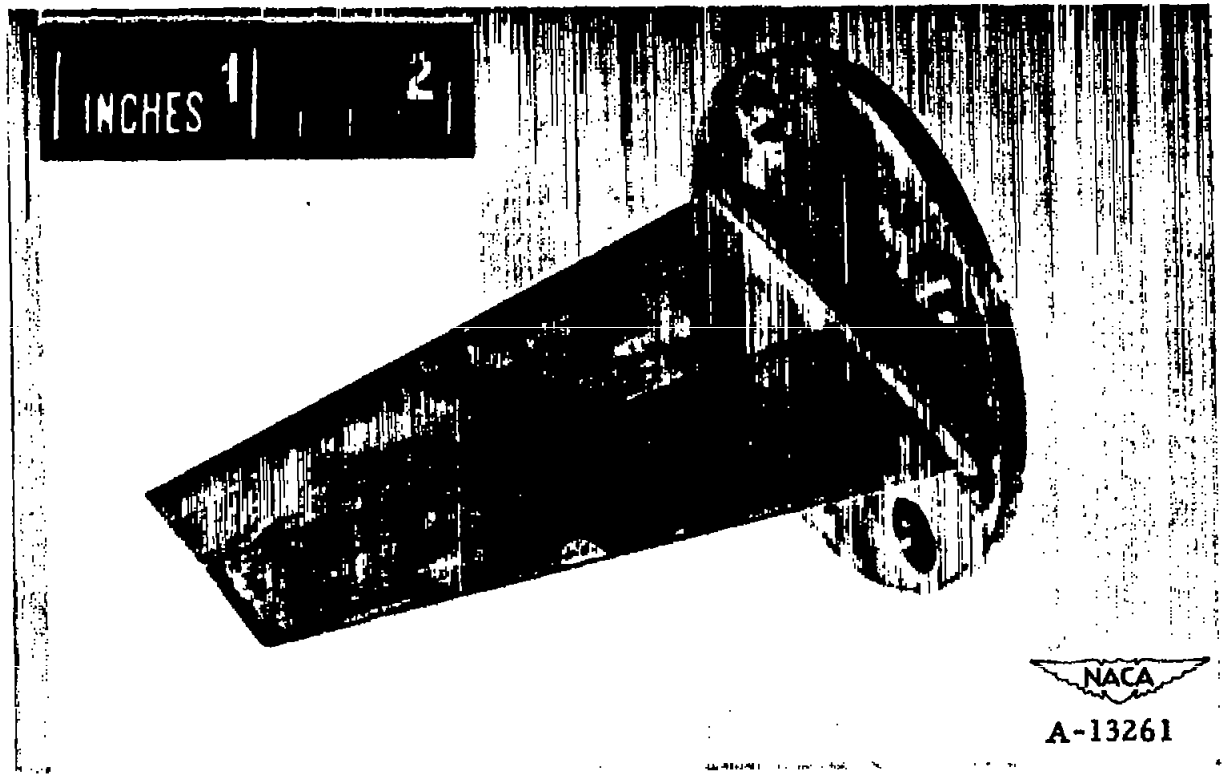

Figure 3.— A photograph of the model tested.

[redacted]

[redacted]

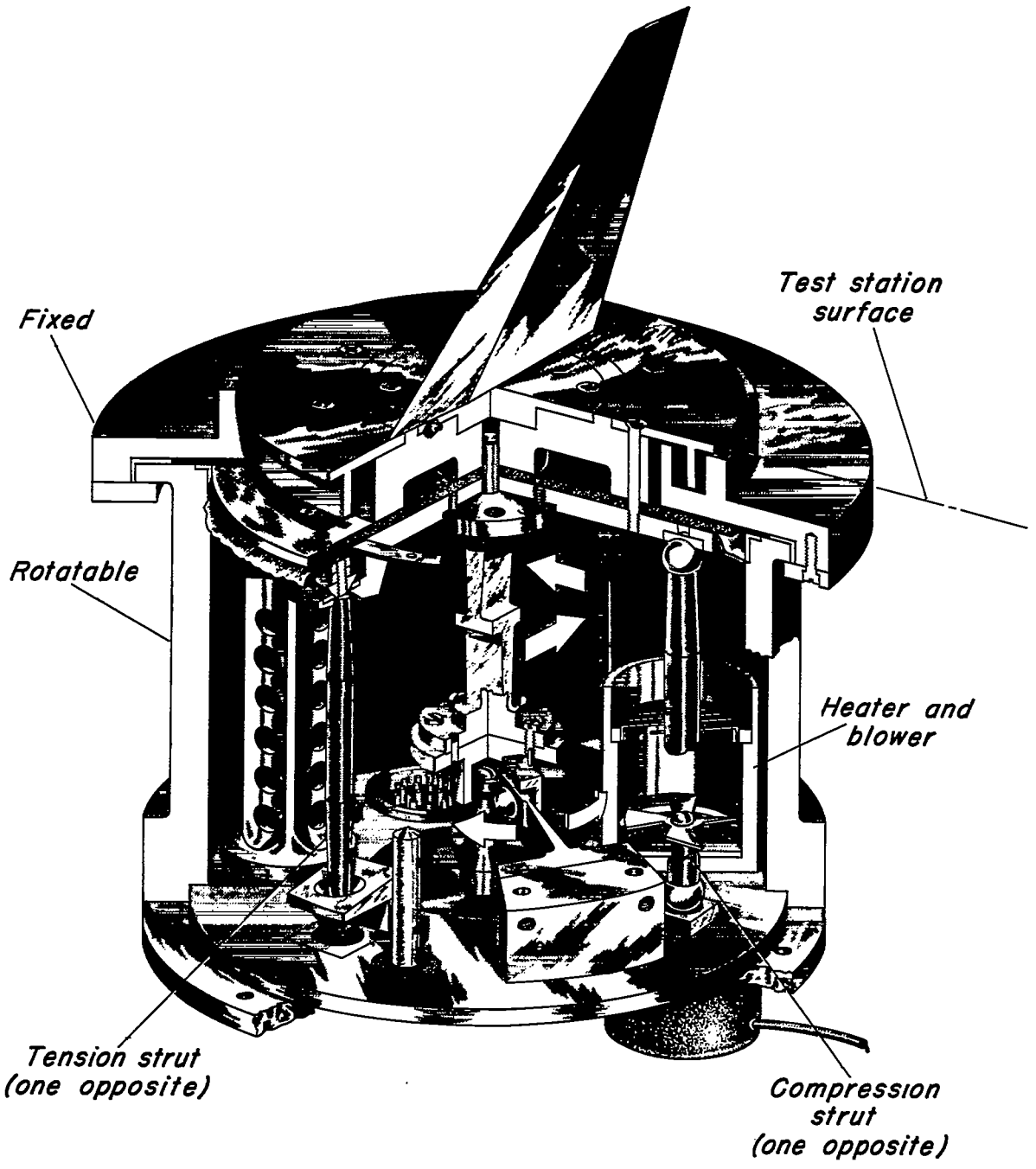

Figure 4.— Three-component test balance.

[redacted]

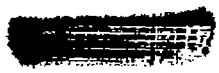

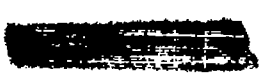

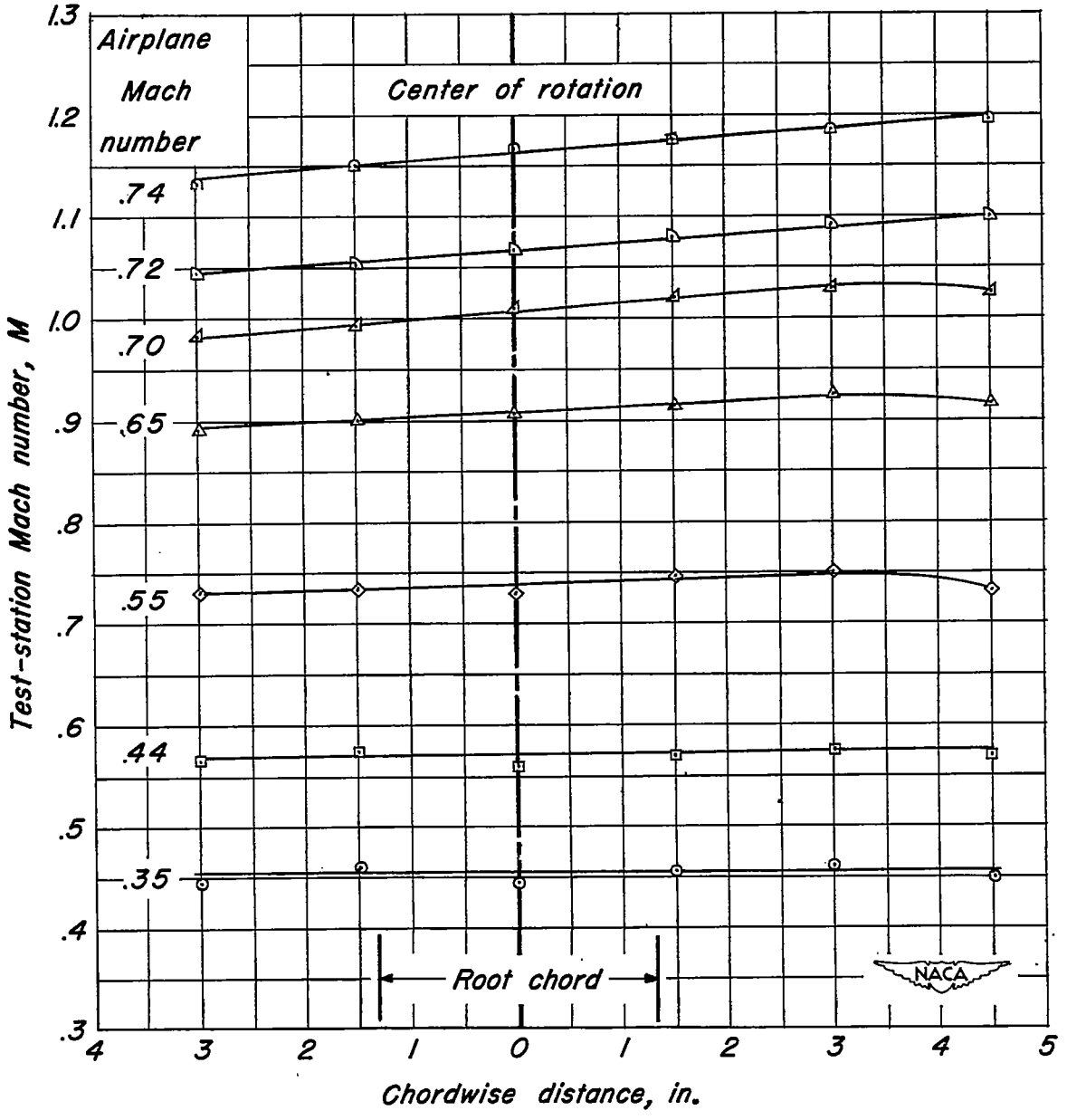

Figure 5.- Streamwise variation of Mach number on wing-flow test-station surface.

[redacted]

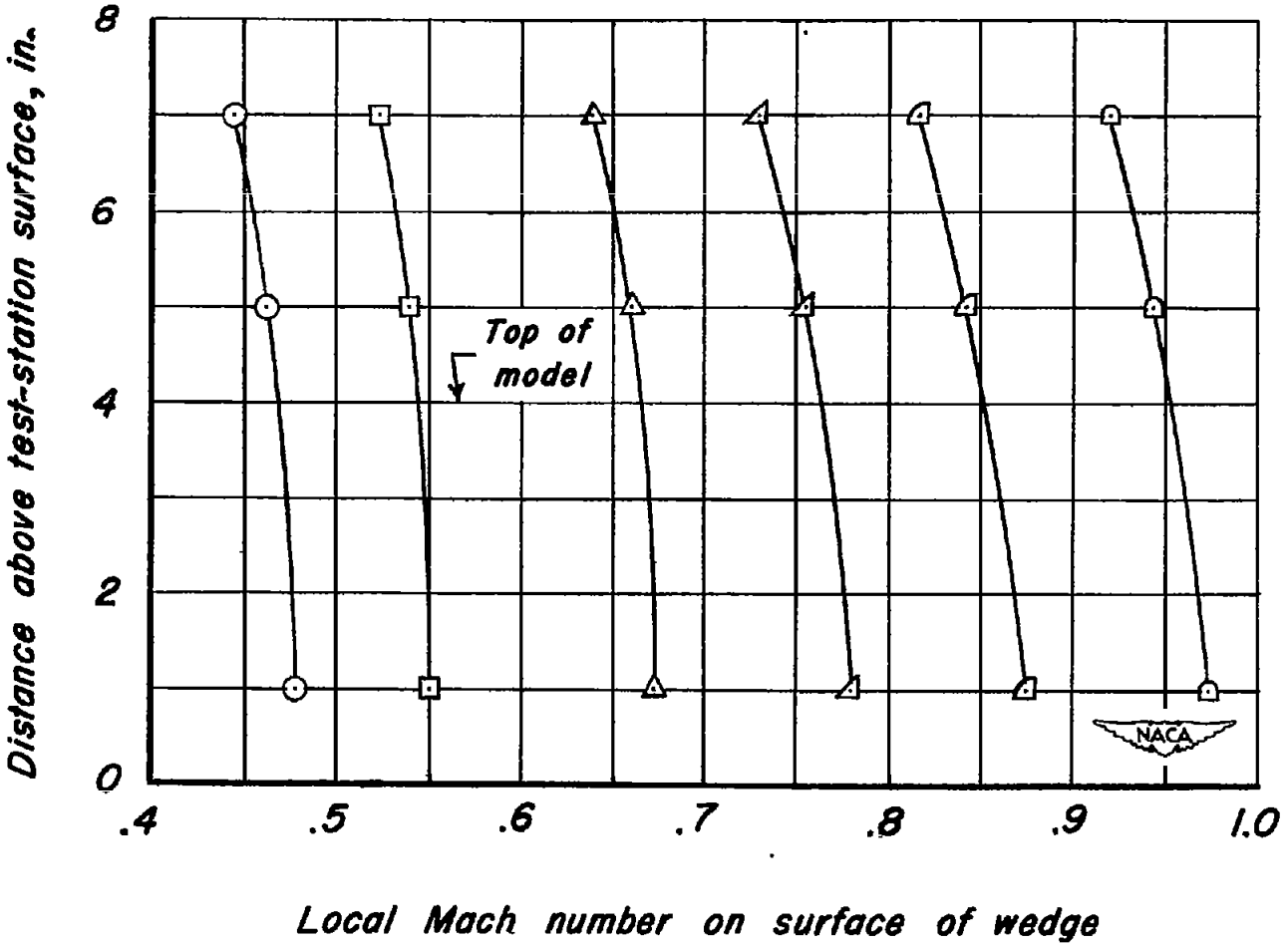

Figure 6.- Typical vertical Mach number distributions obtained by measuring the local Mach number at the 60-percent chord point on a wedge-shaped airfoil mounted on the test station.

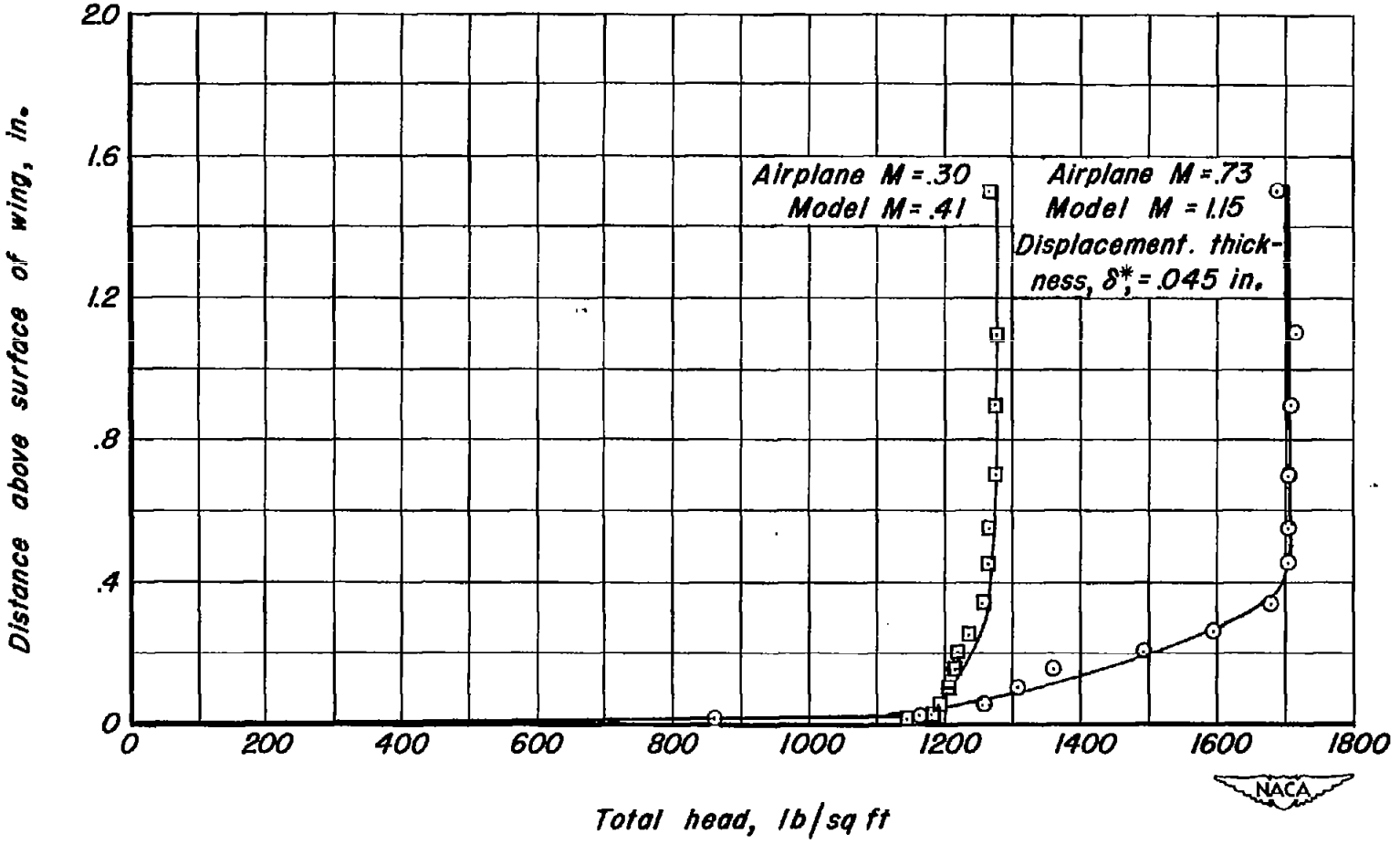

Figure 7.- Typical boundary-layer profiles showing the variation of total pressure on the surface of the wing-flow test station.

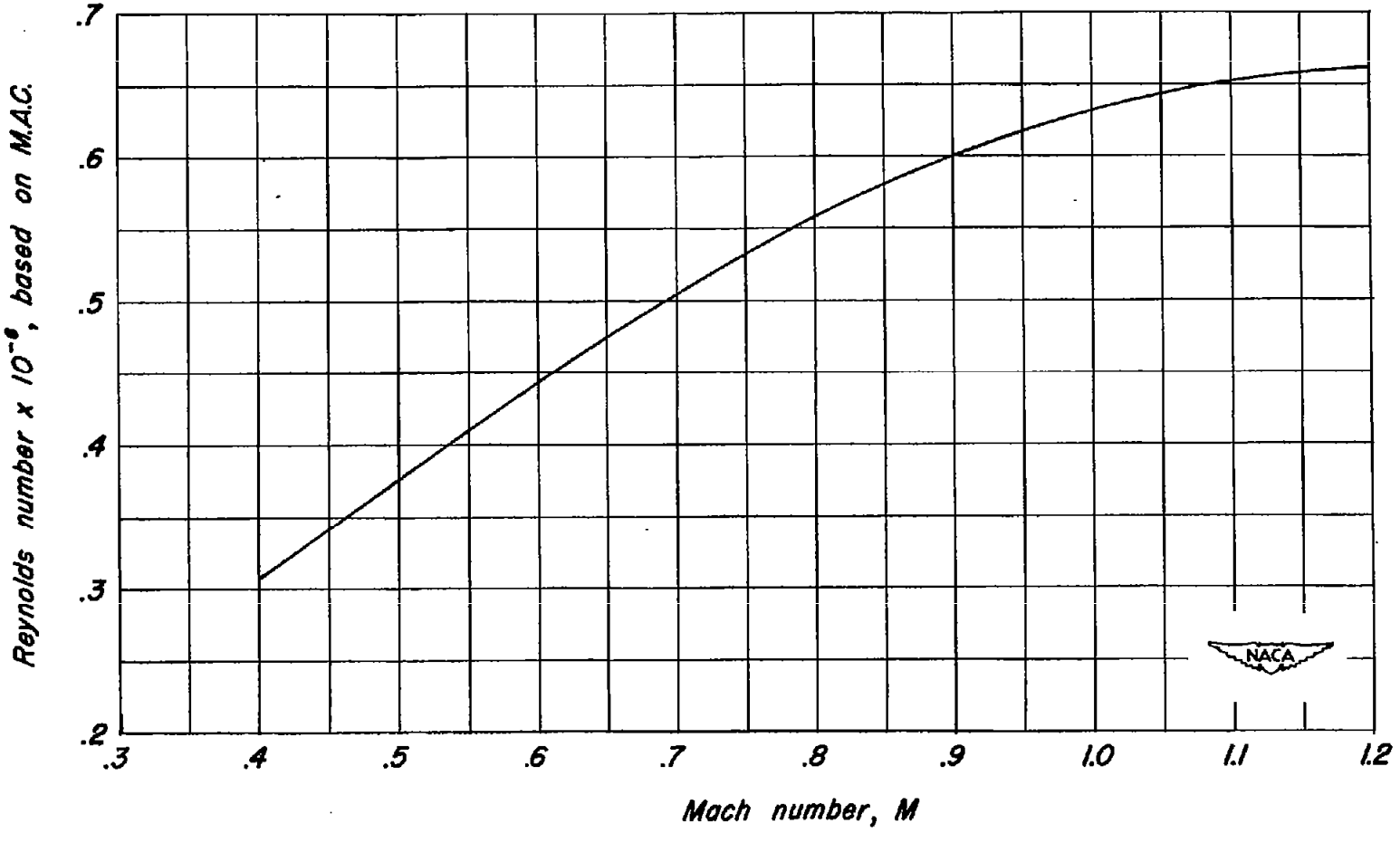

Figure 8.– Variation of Reynolds number with Mach number over the test station.

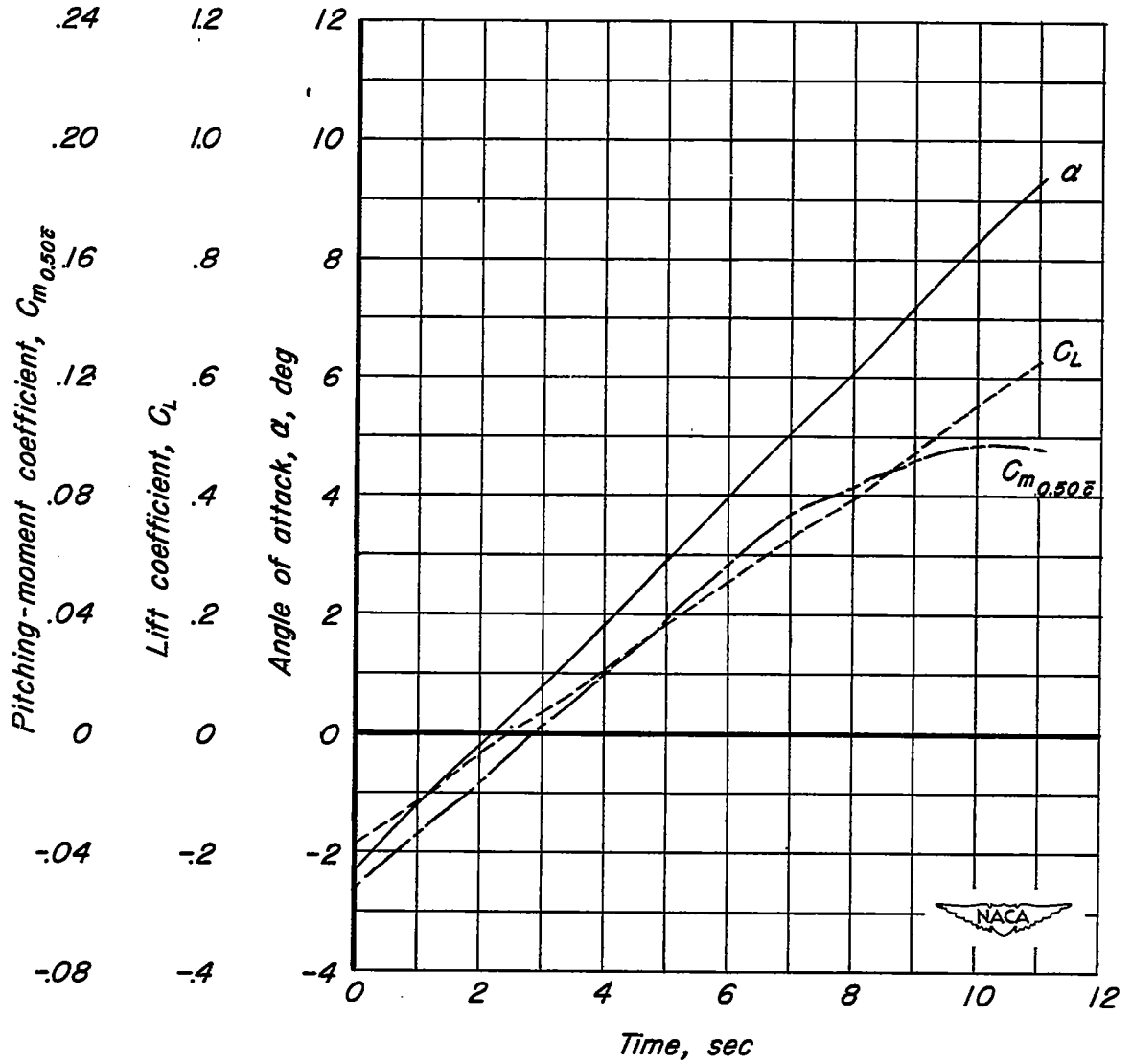

(a) M = 0.51, without lampblack.

Figure 9.- Typical time histories of test data.

[redacted]

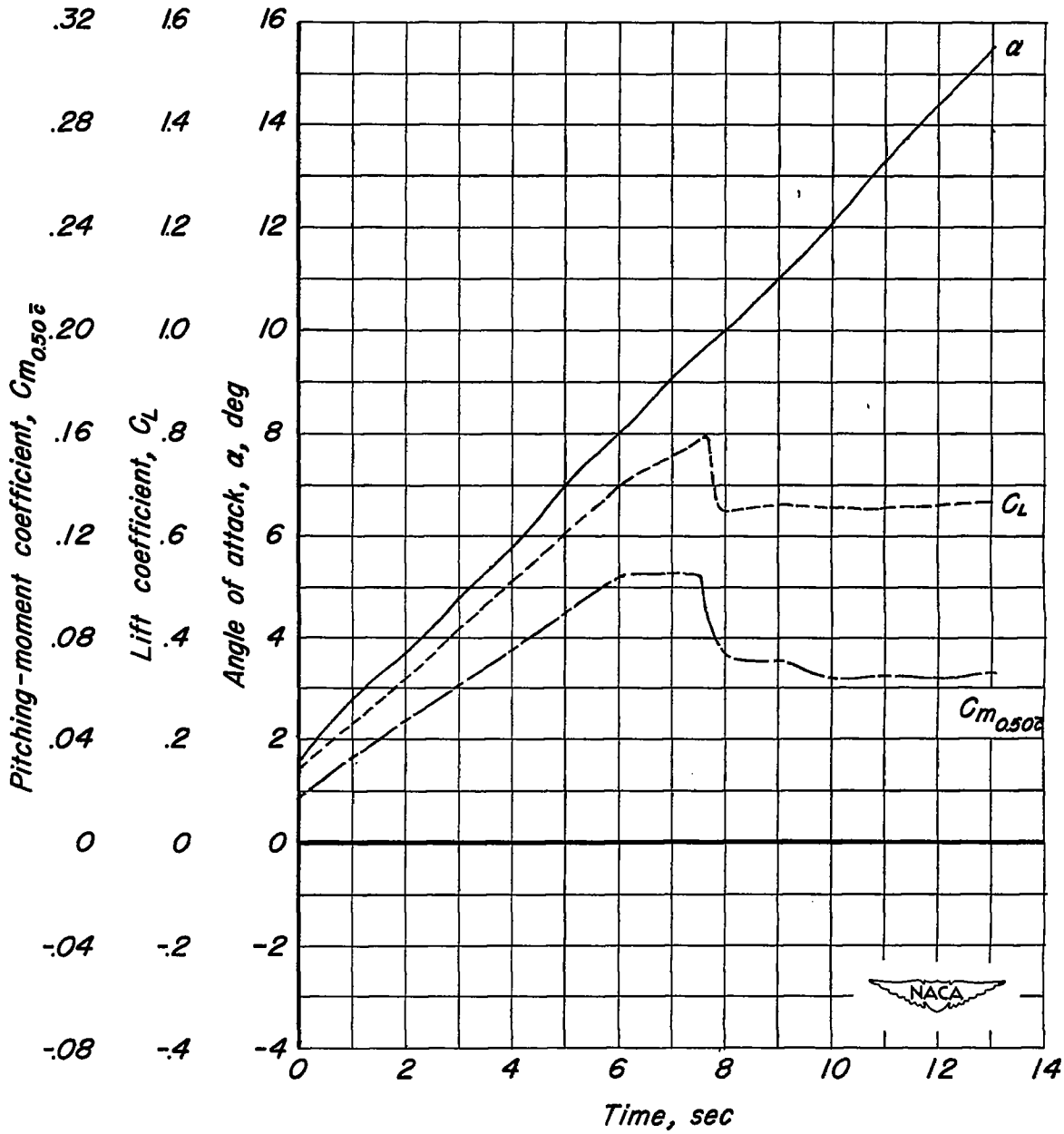

(b) M = 0.88, with lampblack, stall detail.

Figure 9.- Continued.

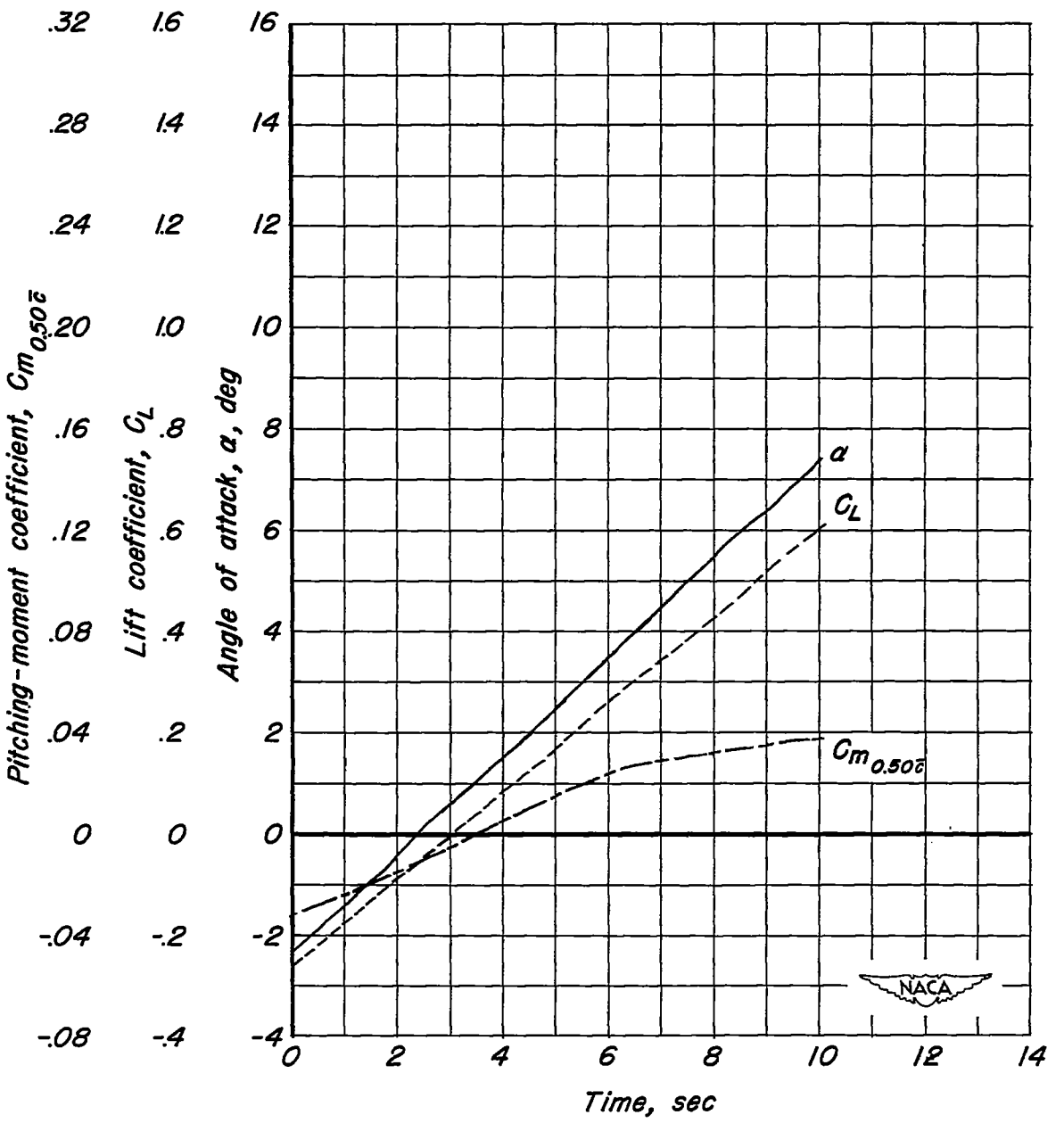

(c) M = 1.11, with lampblack.

Figure 9.- Concluded.

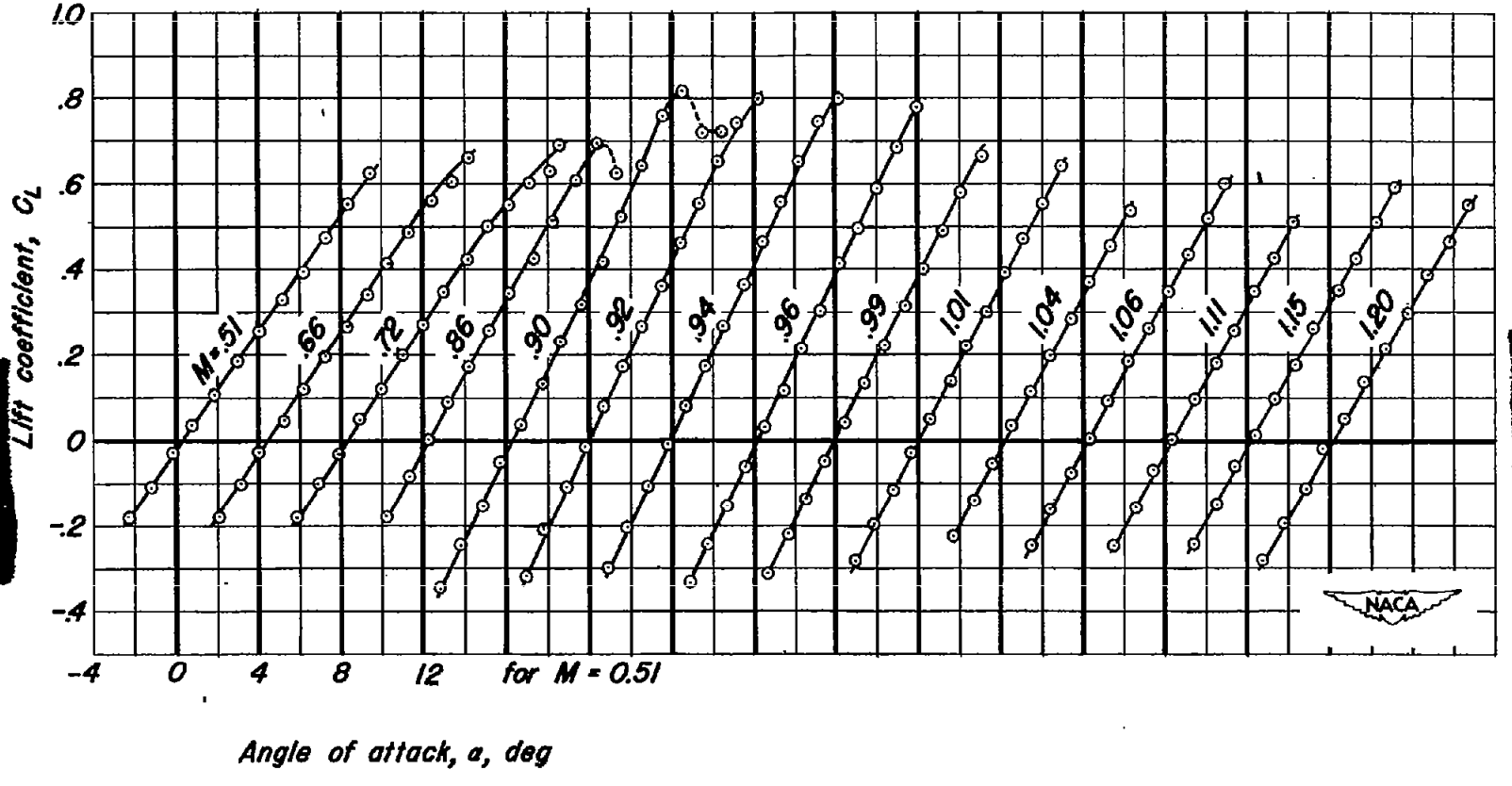

Figure 10.- The variation of lift coefficient with angle of attack at several Mach numbers, model surface polished.

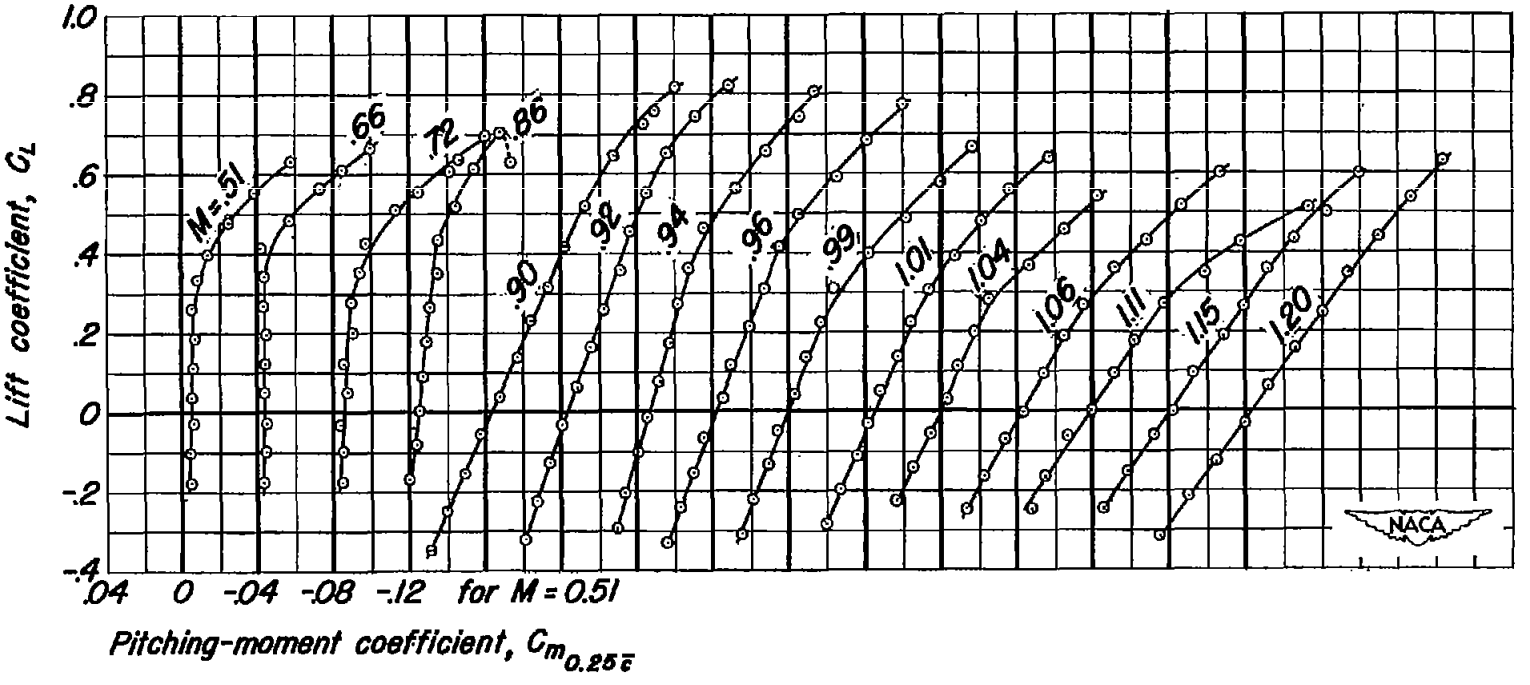

Figure 11.- The variation of pitching-moment coefficient with lift coefficient at several Mach numbers, model surface polished.

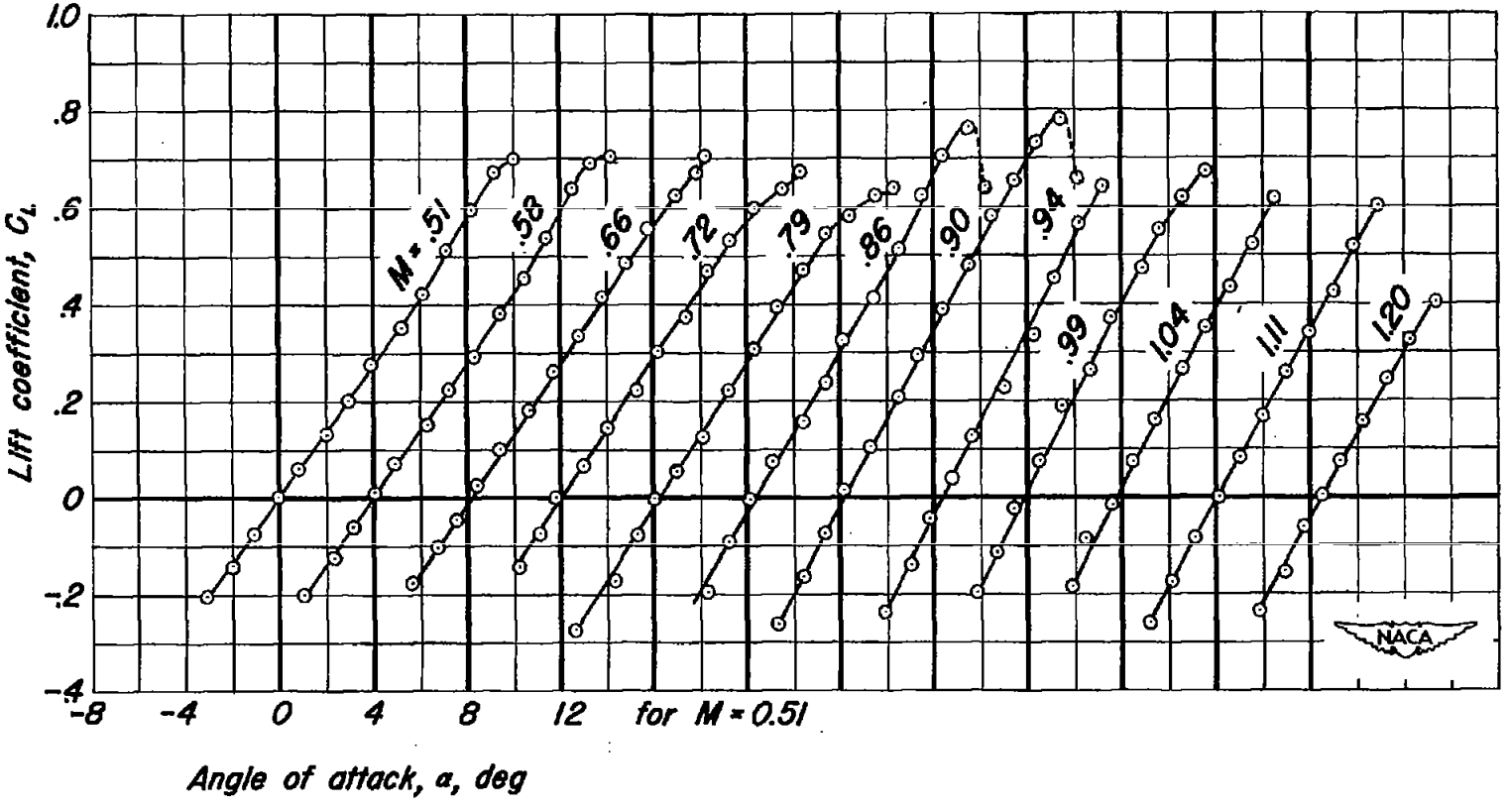

Figure 12.- The variation of lift coefficient with angle of attack at several Mach numbers, model surface coated with lampblack.

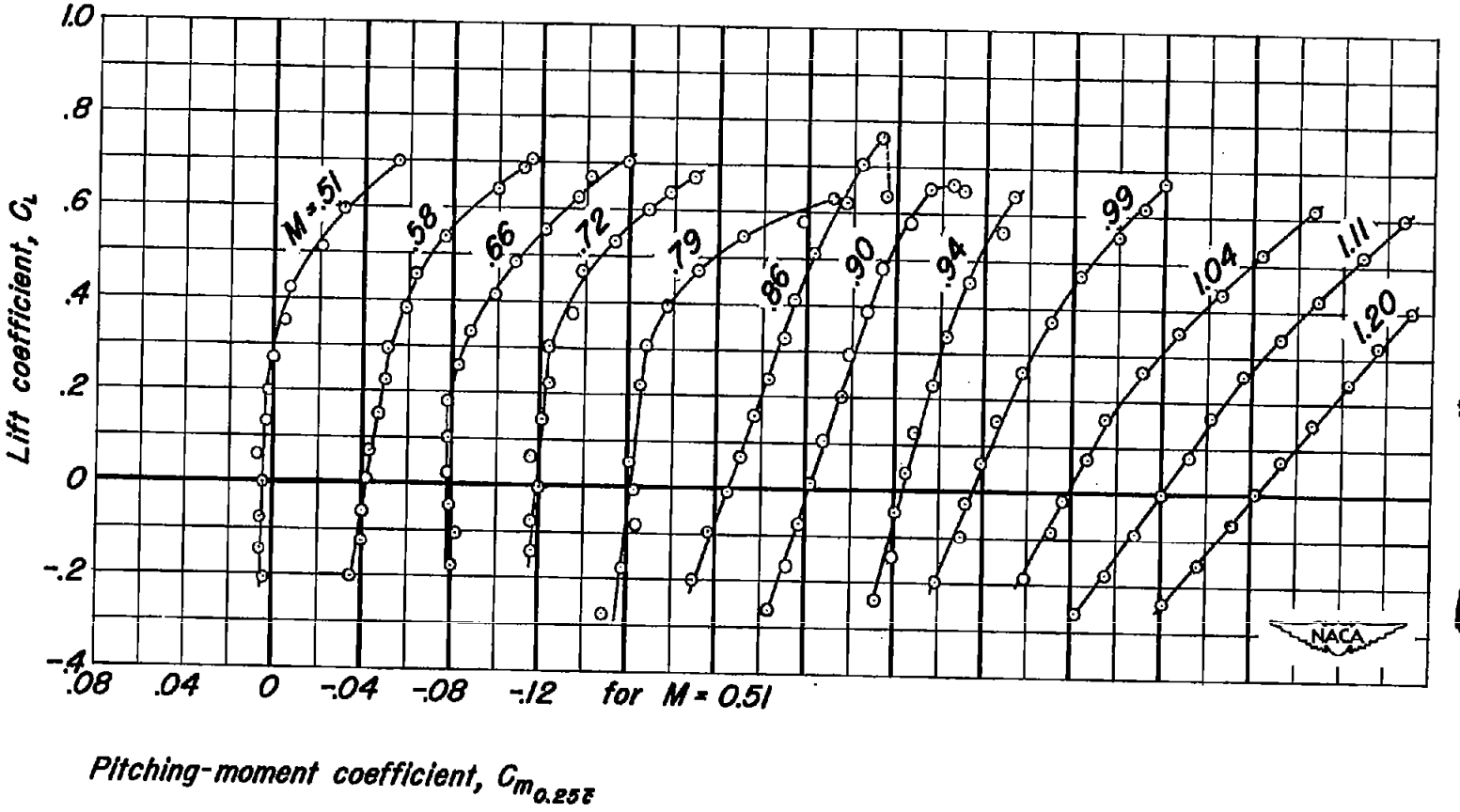

Figure 13.- The variation of pitching-moment coefficient with lift coefficient at several Mach numbers, model surface coated with lampblack.

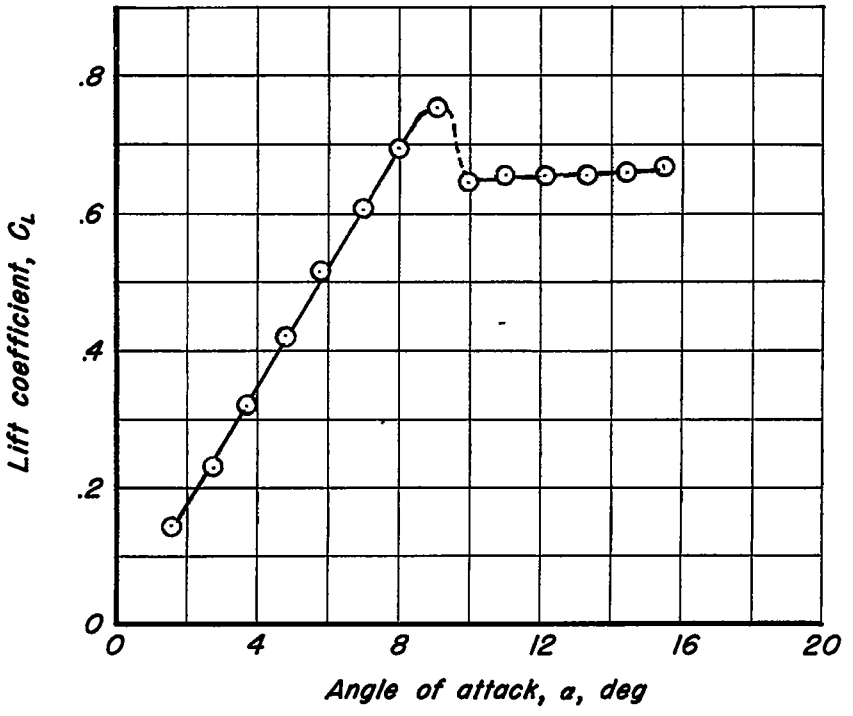

(a) Lift characteristics.

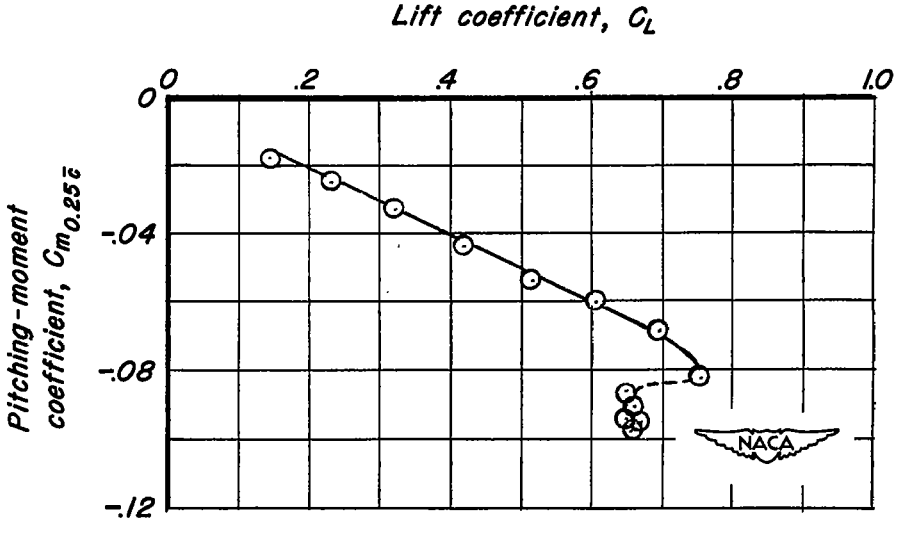

(b) Moment characteristics.

Figure 14.- The characteristics of the wing coated with lampblack during a stall at 0.88 Mach number.

[redacted]

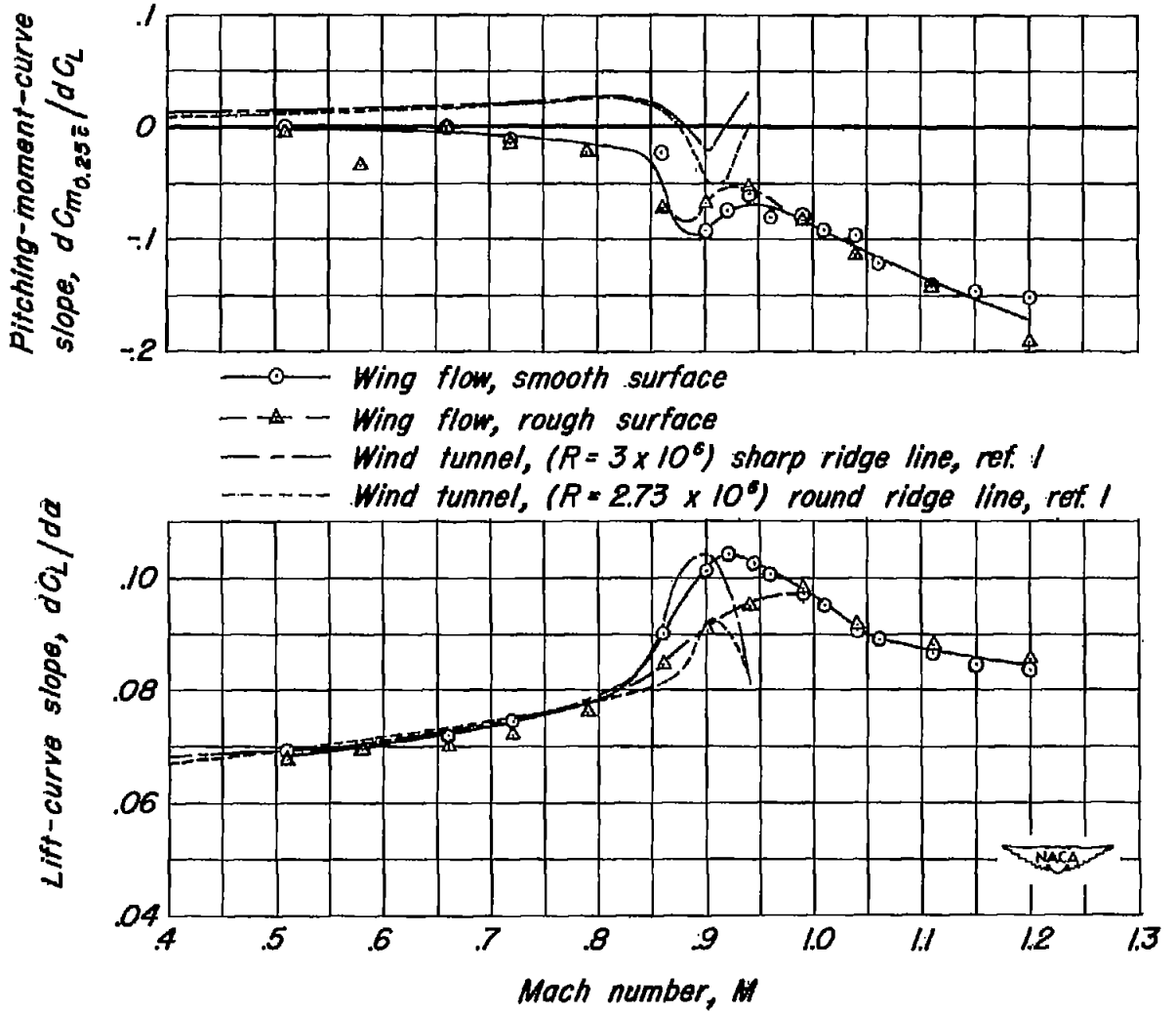

Figure 15.- The effect of Mach number on the lift-curve slope and the pitching-moment-curve slope including comparison with wind-tunnel results.

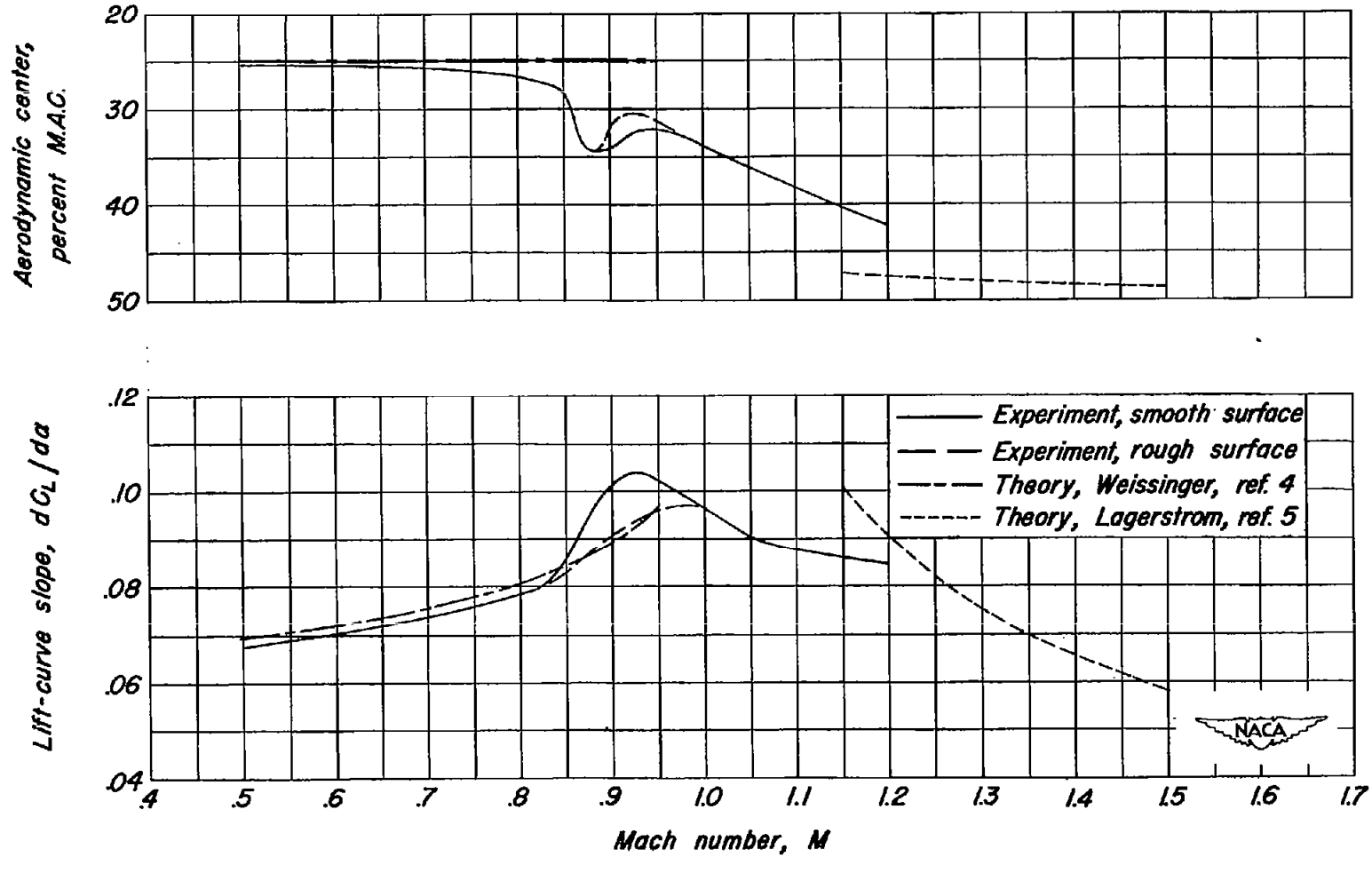

Figure 16.– Comparison of experimental lift-curve slope and aerodynamic center changes due to Mach number with subsonic and supersonic theory.

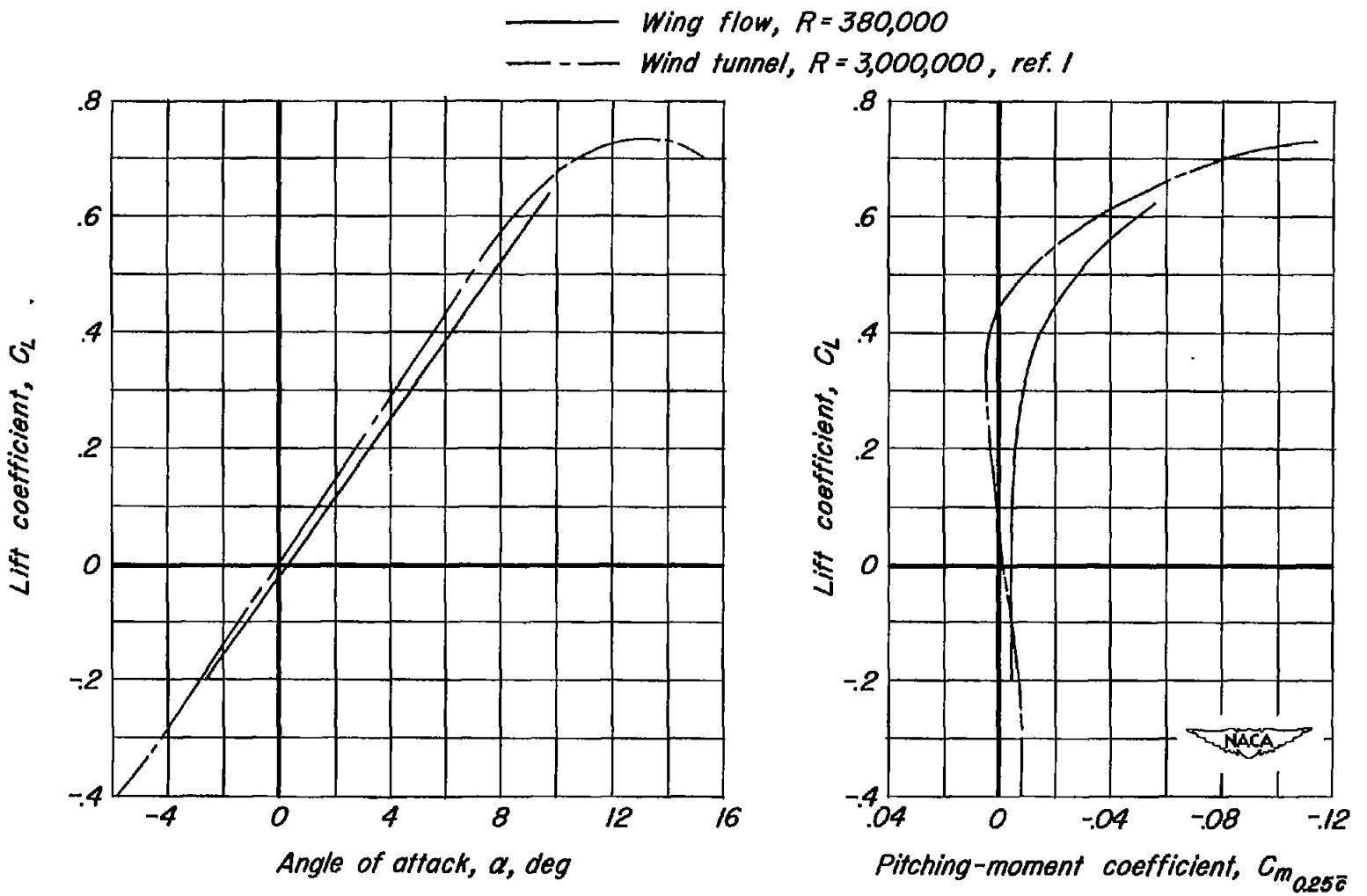

(a) Lift characteristics.

(b) Moment characteristics.

Figure 17.- Comparison of the wing characteristics with sharp ridge line and polished surface as measured in wing-flow and wind-tunnel tests at a Mach number of 0.5.